Prell, W. L., Niitsuma, N., et al., 1991
Proceedings of the Ocean Drilling Program, Scientific Results, Vol. 117

33. PYROLYTIC CHARACTER OF ORGANIC MATTER IN CENOZOIC SEDIMENTS ON THE OMAN SHELF[1]

Kay-Christian Emeis[2, 3] and Jean K. Whelan[2]

ABSTRACT

Analysis of the molecular composition and quantity of pyrolytic hydrocarbons in 41 samples from Owen Ridge and the Oman margin enabled us to identify chemical differences in the organic matter from Owen Ridge and the Oman margin. The differences may be attributed to regional variability in organic matter composition between margin and ridge, effects of kerogen formation and condensation with age, and effects of changes in the depositional environment on the Oman margin. Pyrolytic hydrocarbons from ridge sediments are relatively more enriched in heterocompounds, aromatic molecules, and *n*-alkanes and *n*-monoalkenes in the range *n*-C_9 to *n*-C_{14} when compared to margin sediments. This may be indicative of input of degraded organic material on Owen Ridge and less degraded material on the Oman margin. Increases of long-chain *n*-alkanes and *n*-monoalkenes with depth in sediments from the Oman margin are a result of the concentration of precursor moieties in the kerogen during low-temperature diagenesis. Differences in the depositional environment during deposition of sediments on the Oman margin (changes in the oxygen content of bottom waters and changing benthic activity in a variable oxygen minimum zone) appear to be mirrored in the distribution of monounsaturated isoprenoid hydrocarbons prist-1-ene and prist-2-ene and alkylbenzene.

BACKGROUND AND OBJECTIVES

We examine here chemical differences in organic matter from sediments deposited underneath the monsoonal upwelling system of the northwestern Arabian Sea by pyrolysis and pyrolysis-gas-chromatography/mass spectroscopy. Our first objective was to find molecular criteria that would allow us to distinguish organic matter deposited under anaerobic conditions on the Oman margin, which are laminated, from sediments that are bioturbated and indicate aerobic bottom water conditions. Sediments from the Oman shelf and upper slope are uniquely suited to address the question of differences in organic matter preservation (e.g., Demaison and Moore, 1980; Henrichs and Reeburgh, 1987), because sections recovered at Site 723 on the Oman continental margin (Prell, Niitsuma, et al., 1989) appear to have been deposited under oxic and dysoxic to anoxic conditions in an oxygen minimum zone that changed intensity and/or depth range in the geological past. Analyzing the organic matter composition in sediment intervals deposited under aerobic (bioturbated facies) or anaerobic (laminated facies) conditions may thus provide insight into organic matter composition and rates of decay of compound classes as functions of aerobic and anaerobic bacterial metabolism. We can further calibrate our results using recent surface sediments, for which oxygen levels are known. A second objective was to test whether organic matter character is uniform on the shelf, i.e., underneath the most productive coastal upwelling centers, and the distal Owen Ridge, which has lower accumulation rates of organic carbon and where sedimentation may be strongly influenced by lateral transport from the Oman margin and eolian input.

Study Area

The wind-driven upwelling system of the northwestern Arabian Sea is characterized by seasonal variations in current direction, upwelling intensity, and such biologically important properties of the surface waters as temperature, nutrient content, and primary productivity. Scant productivity data (Wyrtki, 1973) show that upwelling-related productivity during the summer monsoon may exceed 0.5 g C/m^2/day. The combination of high primary production, oxygen consumption, and a lack of advection of oxygenated waters creates a zone of greatly decreased oxygen content that ranges from approximately 150 to 1200 m water depth (Wyrtki, 1973). While the present oxygen levels in the core of the OMZ are sufficient to support benthic activity (D. Anderson, pers. comm. 1989), some Pleistocene and upper Pliocene sediments show laminations that suggest dysaerobic (<0.3 mL/L O_2; Rhoads and Morse, 1971) and possibly anaerobic conditions in the past.

Site 723 (18°03.079′N and 57°36.561′E; Fig. 1) was drilled in water 808 m deep and recovered uppermost Pliocene to Holo-

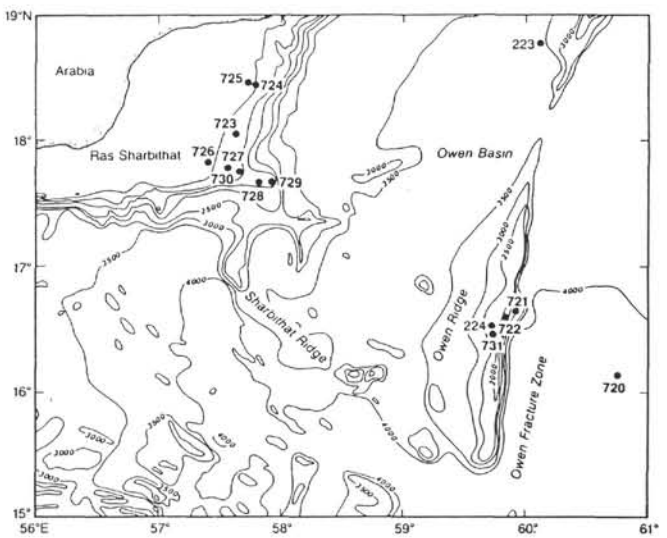

Figure 1. Location map of sites occupied during ODP Leg 117.

[1] Prell, W. L., Niitsuma, N., et al., 1991. *Proc. ODP, Sci. Results,* 117: College Station, TX (Ocean Drilling Program).

[2] Chemistry Department, Woods Hole Oceanographic Institution, Woods Hole, MA 02543, U.S.A.

[3] Current address: Geologisch-Paläontologisches Institut, Olshausenstraße 40, 2300 Kiel, Federal Republic of Germany.

cene(?) foraminifer-bearing nannofossil oozes to calcareous clayey silts. The sedimentation rate is high throughout the section (between 130 and 240 m/m.y.) and the record of variability in eolian and biogenic input during the depositional period is very detailed (Prell, Niitsuma, et al., 1989). Abundance of TOC and the occurrence of laminations in intervals of latest Pliocene to early Pleistocene suggest that bottom-water oxygen contents were lower and precluded bioturbation. Eighteen samples from Hole 723A were used; their depth ranges from 5.9 to 410 mbsf.

Site 728 (17°40.790′N and 57°49.553′E) is located in water 1430 m deep at the lower boundary of the present-day OMZ on the Oman margin (Fig. 1). The recovered section ranges from late Miocene to Holocene in age and sediments are similar in facies than those at Site 723, even though sedimentation rates are significantly lower than at Site 723 (11–90 m/m.y.). Seven samples from this site were analyzed; their depth ranges from 21.4 to 198.8 mbsf.

Surface sediment samples were obtained from box cores retrieved during the 1987 cruise 27 of *Robert Conrad* (Mountain and Prell, 1989) and span the depth interval of the present-day oxygen minimum zone. Bottom-water samples overlying cores RC2714 (590 m water depth), RC2712 (788 m) and RC2723 (815 m), and RC2709 (891 m) had oxygen concentrations of 0.25 mL/L. Carbonate and TOC concentrations of these cores were between 40% and 50%, and 4% to 8%, respectively. Surface sediment from core RC2724 (1400 m) contained 64% $CaCO_3$ and 2.7% TOC, and bottom-water oxygen was measured at 1.0 mL/L (D. Anderson, pers. comm., 1988).

Site 722 is located on Owen Ridge (16°37.312′N and 59°47.755′E) in water 2030 m deep (Fig. 1). The oldest sediments are early Miocene silty claystones, but the dominant lithology is nannofossil ooze to diatomaceous nannofossil ooze with lighter and darker colored alternations on a scale of meters. Coincident with dark colors are TOC concentrations > 2% by weight, and a decrease in $CaCO_3$. Sedimentation rates at Site 722 were between 17 and 54 m/m.y. We studied organic matter character and content in 11 samples spaced across two of the cyclic light-dark intervals in Cores 722A-16X (146–147 mbsf) and 722B-29X (270–271 mbsf).

METHODS

Characterization of organic matter in sediments is made difficult by the fact that condensation reactions during diagenesis lead to the formation of protokerogen and kerogen, which are difficult to study on the molecular level (e.g., Durand, 1980). However, studies of thermally immature and mature sediments have shown that the methods of pyrolysis (in conjunction with gas chromatography/mass spectroscopy) are well suited for the study of these condensed products, which make up more than 80% of sedimentary organic matter (e.g., Durand, 1980). The method of pyrolysis-gas chromatography/mass spectroscopy employed in this study has been used in a number of laboratories mainly in the assessment of hydrocarbon source rocks, but also for differentiating between kerogen types and organic matter characteristics. An overview of the literature on this method is given in Barker and Wang (1988). The pyrolytic approach to compositional discrimination between degraded and undegraded organic matter has been used previously to distinguish aerobic from anaerobic conditions in black shales (Pratt et al., 1986) and in upwelling sediments (Emeis and Morse, 1990; Emeis et al., in press).

The method used in this study is described in detail in Whelan et al. (1990) and Tarafa et al. (1987): 10–30 mg of freeze-dried and ground sediment (after core splitting on *JOIDES Resolution*) is placed in the cooled interface of a Chemical Data Systems (CDS) Model 820 Geological Reaction System and heated at 30°C /min. from 200° to 600°C. Organic compounds desorbed and pyrolyzed during the heating process are swept out of the system in a helium stream. The stream is split three ways: one part goes directly to a flame ionization detector (FID), a second split is trapped for gas chromatography (GC), and a third part is used to characterize the molecular composition of pyrolysates with a GC-mass spectrometer. This experimental setup yields information on molecular composition in addition to the well-known hydrogen indexes (given in mg of pyrolysate/g of TOC). Calibration of GC-amenable components in the pyrolysates is achieved by direct injection of a standard mixture of known composition (toluene, xylenes, and *n*-alkanes from octane to octadecane). The results on compositions and amounts of individual components of pyrolysates are generally highly reproducible; precisions of ± 10% are routinely obtained on resolved capillary GC peaks.

Although catalytic effects at low TOC (below 2 wt%) influence the results of Rock-Eval pyrolysis (e.g., Katz, 1983), we found that catalytic artifacts did not systematically alter the composition of pyrolysates in experiments with bulk sediment and extracted kerogen. A set of five samples (listed in Table 1) was analyzed as bulk sediment and after kerogen preparation. A plot comparing average values of yields from bulk sediment and kerogen shows that the abundances differ after extraction of kerogen, but that the overall distribution patterns are not significantly different (Fig. 2).

Organic carbon (TOC) concentrations were obtained after combustion of acidified samples under helium in a Coulometrics CO_2 Analyzer, and pyrolysis yields were calculated as mg hydrocarbons per g of TOC, the Hydrogen Index (HI). Individual molecular compounds are reported by weight (in ng of thermally evolved compound/mg TOC in GC runs) as detected with a flame-ionization detector.

The total number of peaks (and compounds) in each gas chromatogram is beyond the number of parameters that can reasonably be monitored and compared between samples without the aid of automated data collection and reduction via computer. We selected and quantified 32 compounds in the gas chromatogram of each sample. They encompass the dominant contributors to the resolved pyrolysates (skewed toward hydrocarbons, which are the dominant compounds) and were further selected to include examples of each major compound class present in the pyrolysate (Fig. 3). The sum of these 32 compounds is between 17% and 39% of the resolved pyrolysis yield in the samples studied here. The data matrix was used as input for multivariate data analysis (factor analysis and VARIMAX rotation) with the SYSTAT package on an Apple Macintosh.

RESULTS AND DISCUSSION

Four kerogen preparations of samples from Hole 723A and a kerogen of organic-lean marl (TOC < 0.1%) from Hole 722A were examined by fluorescent and reflected-light microscopy (D. I. O'Connor, pers. comm., 1989; Table 1). All samples from Site 723 had very similar kerogen characteristics, and organic matter was dominantly composed of marine macerals, i.e., amorphous and exinitic matter, which together accounted for more than 90% of the particles. Land-derived material, i.e., vitrinite, was less than 10%. Inertinitic, or residual charcoal-like material, accounted for less than 5% in the samples. The one sample of organic-lean marl from Site 722 contained very little kerogen, as is typical for deep-sea sediments deposited under oxic bottom-water conditions, and vitrinite and inertinite are relatively more abundant than in the margin samples. They constitute residual, reworked organic matter, and possibly a higher contribution by wind-blown terrigenous particles.

In the light of the dominantly marine organic matter in sediments from margin and ridge, the yield of pyrolyzable hydrocarbons per g of TOC (the hydrogen index, HI) of both margin

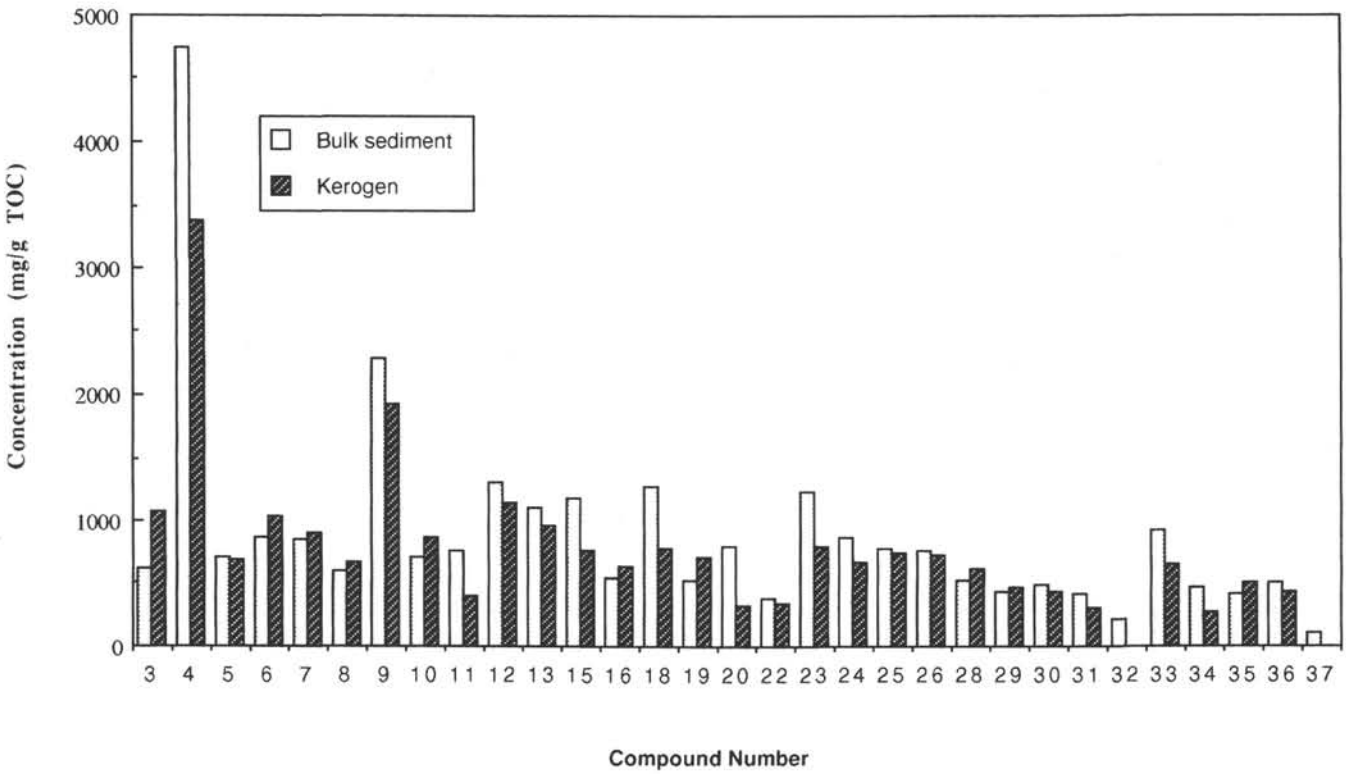

Figure 2. Plot of average yields of pyrolytic hydrocarbons for five bulk samples and corresponding kerogens. Numbers on X-axis are keyed to compounds from Table 3. Note that the abundances may change due to the chemical preparation of kerogens, but that the compositional patterns are the same.

and ridge samples was thus expected to follow the line of marine type II organic matter (Espitalié et al., 1977). Figure 4 is a representation of oxygen and hydrogen indexes of the samples from Oman margin Sites 722, 723, and 728 studied onboard the *JOIDES Resolution* (Prell, Niitsuma, et al., 1989). The oxygen and hydrogen indexes of samples from Sites 723 and 728 plot between the evolution path of marine type II and terrestrial type III organic matter. The shift toward more oxygen-rich type III may be attributable to the presence of oxygen-rich organic matter and possibly to thermal decomposition of carbonate minerals in these immature and carbonate-rich sediments. Even though we cannot rule out that mineral matrix effects, e.g., contribution of CO_2 from pyrolytic carbonate decarboxylation, contribute to the elevated OI of the samples from the Owen Ridge, we take the significantly higher OI in these samples as an indication of different composition of organic matter. For this we have two reasons: the sediments of the Oman margin (Site 723) contain roughly the same amount and compositional assemblage of siliciclastic material as does the Owen Ridge sediment, and $CaCO_3$ concentrations in excess of 50% on the margin vs. 60%–70% on Owen Ridge cannot explain the significant differences in pyrolytic CO_2 yield from mineral decomposition.

Molecular Composition of Pyrolysates

If different depositional conditions indeed influence the preservation of labile components of organic matter, as was proposed by Demaison and Moore (1980), we would expect to find a difference in the character and amounts of compounds that are released from sediments of different facies during pyrolysis. We should thus be able to identify indicators for preservation and different sources of organic matter in the pyrolysate.

Figure 3 shows a typical example of a reconstructed ion chromatogram of the total pyrolysate of Sample 723A-1H-4, 145–150 cm (5.9 mbsf), obtained from gas-chromatography/mass spectrometry of pyrolysis products. Comparison of mass spectra of each peak with library spectra and with spectra of standards enables us to determine the molecular nature of these peaks. Once identified, the abundance of selected molecules (numbers keyed to Table 2) can be quantified on GC traces of all samples.

One prominent feature of the pyrolytic hydrocarbon fraction of all samples studied are the doublets of alkanes and alk-1-enes that extend from carbon chains of 8 carbon atoms to well beyond 20 carbon atoms. In every type II kerogen, these straight-chain alkyl molecules appear to be important contributors to the pyrolysis products. Although their origin is not clear, they are thought to have a significant lipid contribution and to be precursor molecules in kerogen that yield hydrocarbons in petroleum during catagenesis (e.g., van de Meent et al., 1980). Nip et al. (1986) proposed that the precursors of alkane-alkene doublets are nonsaponifyable, highly resistant biopolymers that are very stable under any depositional conditions. They are believed to be highly aliphatic macromolecules with long polyalkyl (polymethylene) chains as major structural elements (Tegelaar et al., 1989). In addition to the normal alkanes and alkenes, we recognize substantial contributions of branched, aromatic, cyclic, and heterocompounds (containing O, N, and S) in the pyrolysates. Polyunsaturated alkyl hydrocarbons were not observed in the pyrolysates.

Statistical Evaluation of Molecular Character

The data matrix of 32 parameters from 41 samples was treated by statistical factor analysis (Table 3). We thus singled out those parameters that contribute most to the variance in the data and were able to compute factors (composites of parameters) that enable us to discriminate between samples (Howarth

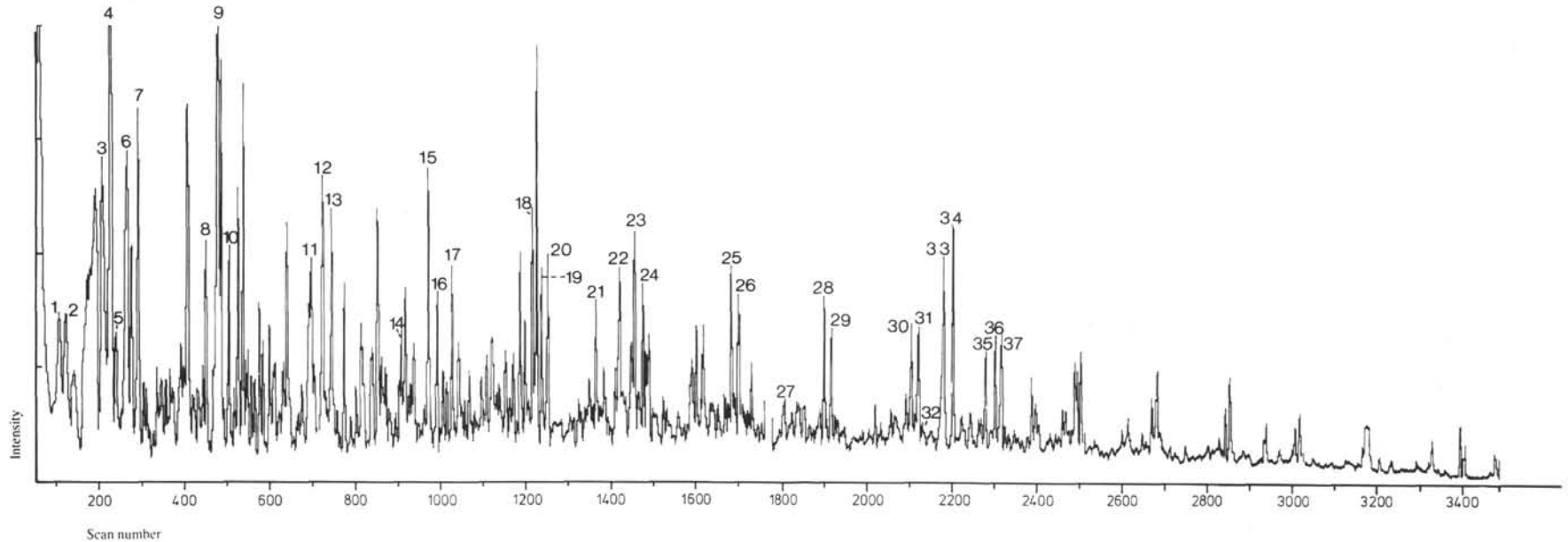

Figure 3. Reconstructed ion chromatogram of pyrolyzed organic compounds from Sample 723A-1H-4, 145–150 cm (5.9 mbsf). Examples of the most abundant compounds recognized from mass spectra are indicated. Quantification of compounds labelled 1 through 37 and listed in Table 3 was performed by gas chromatography.

Table 1. Petrography of kerogen concentrates from Sites 723 and 722.

Sample	Description	Kerogen type Amorphous	Exinite	Vitrinite	Inertinite	Bituminite
723A-1H-4, 145–150 cm	Light golden brown, fluffy amorphous algal material. Exinite and vitrinite fragments present, but oxidized and rough.	80	10	5	5	0
723A-9H-4, 145–150 cm	As above	80	10	Tr	5	5(?)
723A-13X-4, 145–150 cm	As above	90	10	Tr	Tr	0
723A-29X-6, 145–150 cm	As above	90	10	0	Tr	0
722A-22X-4, 145–150 cm	As above, relatively more inertinite	60	10	15	15	0

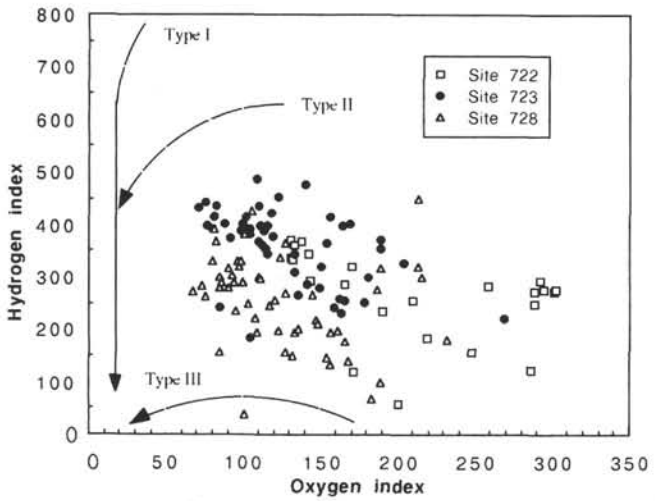

Figure 4. Plot of Hydrogen Index and Oxygen Index for samples from Sites 722, 723, and 728. Curved lines represent empirical compositions of type I (brackish) type II (marine) and type III (terrestrial) organic matter. Data from Prell, Niitsuma, et al. (1989).

and Sinding-Larsen, 1983). A similar approach has been used with good success by Øygard et al. (1988) on pyrolysates of kerogen samples from wells on the continental shelf of Norway. The result of the first step, the evaluation of parameters for their contribution to the variance in the entire data set, revealed that three factors contribute 80% to the variance, with factor 1 the most dominant contributor (43% of variance after rotation). Factor 1 is predominantly loaded with contributions from aromatic and heteromolecules (naphthalenes, thiophenes), and from short-chain hydrocarbons (9–15 carbon atoms). Factor 2 (25% of the variance) is dominated by straight-chain saturated and monounsaturated hydrocarbons (16–18 carbon atoms) and isoprenoids pristane and phytane. Factor 3 (11% of the variance) is dominated by alkylbenzene, and monounsaturated isoprenoids prist-1-ene and prist-2-ene (Table 2).

If we plot the scores of all samples on factors 1 and 2, we achieve a separation of samples from the Owen Ridge (Site 722) and samples from the margin (Fig. 5, top). The separation between samples from the margin and the ridge is mainly based on scores of samples on factor 1 (dominated by short hydrocarbon chains, heterocompounds, and aromatic molecules). Pyrolysates of sediments from the ridge is thus richer in these molecules per g of TOC than kerogen on the margin. On the other hand, samples from surface cores have the most negative scores on factor 1, which means that short-chain, aromatic, and heterocompounds are least abundant in organic matter from surface sediments on the Oman margin.

Table 2. List of compounds quantified in the pyrolysates and shown as numbers on Figure 3. Factor loadings for factors 1 to 3 are added.

Peak number in Figure 5	Compound	Loading on Factor 1	Factor 2	Factor 3
1	Octene			
2	Octane			
3	2,4 (dimethy)-(1H)-pyrrole	−0.048	0.500	0.127
4	Dimethylbenzene	0.660	0.083	0.592
5	2,3-dimethylthiophene	0.910	−0.098	0.269
6	Nonene	0.845	0.221	0.100
7	Nonane	0.809	−0.056	0.373
8	2,3,4-trimethylthiophene	0.623	0.027	0.551
9	1-ethyl-2-methylbenzene	0.468	0.104	0.810
10	Decane	0.899	−0.233	−0.106
11	1-methylphenol	0.827	0.125	0.070
12	Undecene	0.856	0.167	−0.059
13	Undecane	0.786	0.180	0.409
14	1-methylindene			
15	Dodecene	0.867	0.274	0.078
16	Dodecane	0.858	0.153	0.281
17	2,6-dimethyl undecane			
18	Tridecene	0.760	0.367	−0.093
19	Tridecane	0.623	0.334	0.188
20	1-methylnaphthalene	0.929	0.084	0.245
21	2,6,11-trimethyl dodecane			
22	Benzothiophene	0.929	−0.016	0.186
23	Tetradecene	0.874	0.333	−0.039
24	Tetradecane	0.814	0.365	0.370
25	Pentadecene	0.767	0.522	0.239
26	Pentadecane	0.666	0.491	0.390
27	Alkylbenzene			
28	Hexadecene	0.158	0.909	0.070
29	Hexadecane	0.161	0.957	0.046
30	Heptadecene	0.085	0.880	0.001
31	Heptadecane	0.140	0.913	0.044
32	Pristane	0.146	0.847	0.218
33	Prist-1-ene	−0.144	0.433	0.703
34	Prist-2-ene	0.428	0.262	0.632
35	Octadecane	0.068	0.908	0.014
36	Octadecene	0.022	0.789	0.318
37	Phytane	0.047	0.770	0.126

Factor 2 (the amount of saturated and monounsaturated alkyl chains [16–18 carbon atoms] and isoprenoids pristane and phytane normalized to TOC) has no obvious correlation with the depositional environment on margin or ridge (Fig. 5, top), because scores on factor 2 are evenly distributed over margin and ridge samples alike. The scores of surface sediments on this factor are in the lower range of all samples, but overlap with those of all other samples. We consider this as an indication that the concentrations of the compounds that compose factor 2 is independent of organic matter quality and amount, as well as of depositional environment.

From the clusters of samples in Figure 5 (bottom), which plots cores of factor 1 against factor 3, it appears that samples from Sites 723 and 728 contain relatively more alkylbenzene and long-chain isoprenoid hydrocarbons (prist-1-ene and prist-2-ene;

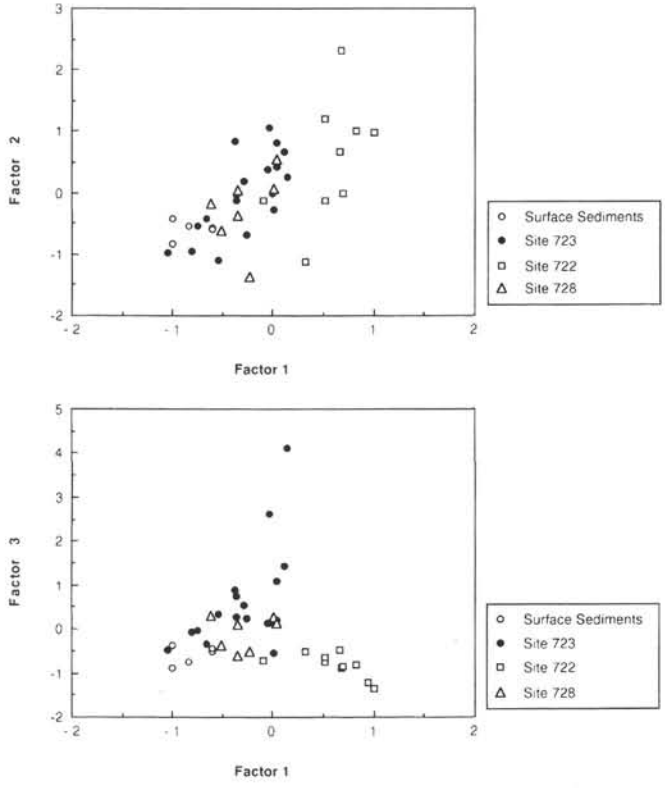

Figure 5. Plot of factor scores of samples on factors 1 and 2 (top) and factors 1 and 3 (bottom) extracted from the data matrix of 41 samples from Oman margin sediments. Note the separation of samples from Site 722. Factor 1 is dominated by concentrations of aromatic and heterocompounds (naphthalenes, thiophenes) and short-chain alkyl molecules (C_{10} to C_{15}), while factor 2 is dominated by straight-chain and branched alkanes and olefins of 16–20 carbon atoms. Factor 3 has highest contributions from alkylbenzene and unsaturated branched alkanes (prist-1-ene, prist-2-ene) (compare Table 3).

factor 3) in their pyrolysates than either samples from the Owen Ridge (Site 722) and the surface sediments samples from the Oman margin. The amount of organic carbon has no influence on this relationship, but it is of note that highest scores on factor 3 occur in sediments of Site 723 in which laminations and opaline microfossils are preserved.

To distinguish any effect of burial diagenesis and variable depositional conditions through time on the moieties that compose factors 1 to 3, we plotted depth profiles of factor scores (Fig. 6) for the sediments from margin Sites 723, 728, and surface sediments. In addition, we plotted the sum of the quantified hydrocarbons (in mg/g TOC), which is a "defined" hydrogen index (Fig. 6A). To discern any effect of bottom-water oxygenation (indicated by the presence of laminations) on the composition of pyrolysates in samples from Site 723, we marked the depth range of the organic-rich and partly laminated interval deposited around the Pliocene/Pleistocene boundary at that site.

No consistent changes with depth are discernable in scores on factor 1, the factor representing pyrolysates relatively enriched in aromatic and heterocompounds that we interpret to be indicative of degraded organic matter. Surface sediments have low scores on this factor (Fig. 6B), and variability in all margin sediments is rather low. Factor 2, however, which combines long-chain hydrocarbons, shows an increase with depth from surface sediments to the deeper samples of Site 723. We take the increase of factor 2 with depth to indicate that the concentration of those kerogen moieties which yield long-chain *n*-alkyl pyrolysate are preferentially enriched in the organic matter with depth in the sediment (and thus with time; Fig. 6C). This relation holds for sediments from surface sediments and both Sites 723 and 728, and is in keeping with the hypothesis of a preferential preservation of a highly resistant, aliphatic, macromolecular precursor substance (algaenan; Tegelaar et al., 1989) in sedimentary organic matter that undergoes continuous biodegradation during anaerobic diagenesis.

A pronounced increase of scores on factor 3 and of the sum of quantified hydrocarbons shown in Figure 6A is obvious in sediments from the sediment interval containing laminations at Site 723 (Fig. 6C). Kerogen moieties that yield prist-enes and methylbenzene upon pyrolysis are thus significantly enriched in the sediments deposited under conditions of impeded benthic activity. Van de Meent et al. (1980) believe that chlorophyll is the biological source of the sedimentary precursor substance that yields isoprenoid hydrocarbons prist-1-ene and prist-2-ene upon pyrolysis. According to the results of Goossens et al. (1984), other likely precursor substances are tocopherols. With the data at hand, we can draw the conclusion that the precursor substance of prist-enes and alkylbenzene is preferentially preserved in sediments that were deposited under low oxygen or even anoxic conditions at the sediment-water interface, without being able to decide the origin of these abundant pyrolysis products.

CONCLUSIONS

1. The main variability in this dataset is the difference between pyrolysates from sediments underneath upwelling cells and those that were deposited several hundreds of miles offshore on Owen Ridge. The latter contain more heterocompounds, and alkane/alkene doublets in the range from C_9 to C_{14}. In light of the predominance of marine organic matter at all locations studied, we suggest that the observed differences, notably the abundance of aromatic molecules and heterocompounds, are related to the degree of reworking prior to deposition.

2. Individual molecular building blocks of kerogen or humus are preferentially enriched during diagenesis in our samples. The amount of long-chain alkane/alkene doublets (range from C_{16} to C_{18}) relative to TOC increases with depth at the Oman Margin sites.

3. If we use the macroscopic facies differences of bioturbation vs. lamination as a guideline for determining past extents and intensities of the oxygen minimum zone on the Oman shelf, our attempt to chemically distinguish sediments from anaerobic and aerobic depositional conditions was successful, if somewhat ambiguous. Specific groups of pyrolyzable compounds, namely those that yield monounsaturated isoprenoid hydrocarbons prist-1-ene and prist-2-ene and alkylbenzene appear to be enriched in samples with high HI, and may be indicative of molecular differences in sedimentary organic matter from the two types of environments.

ACKNOWLEDGMENTS

We thank Martha Tarafa and Peggy Dickinson for analytical help, and Carl Johnson for assistance with the mass spectroscopy. Dave Anderson, Mark McCaffrey, John Farrington, and Remy Hennet provided valuable samples, discussion, comments, and data. The authors gratefully acknowledge financial support by USSAC and Shell Development Company, and technical support by the Ocean Drilling Program. This work was supported by the National Science Foundation, Grant No. OCE 85-09859. This is Woods Hole Oceanographic Institution contribution No. 7527.

REFERENCES

Barker, C., and Wang, L., 1988. Applications of pyrolysis in petroleum geochemistry: a bibliography. *J. Anal. Appl. Pyrol.,* 13:9–61.

Demaison, G. J., and Moore, G. T., 1980. Anoxic environments and oil source bed genesis. *Org. Geochem.,* 2, 9–31.

Durand, B., 1980. *Kerogen.* Paris (Editions Technip).

Emeis, K.-C., and Morse, J. W., 1990. Relationship of organic carbon to sulfur in sediments from the Peru margin, ODP Sites 680 and 688. *In* Suess, E., von Huene, R., et al., *Proc. ODP, Sci. Results,* 112. College Station, TX (Ocean Drilling Program), 441–453.

Emeis, K.-C., Whelan, J. K., and Tarafa, M., in press. Sedimentary and geochemical expression of oxic and anoxic conditions on the Peru shelf. *In* Tyson, R., and Pearson, T. (Eds.) *Continental Shelf Anoxia.* Geol. Soc. London Spec. Publ.

Espitalié, J., Laporte, J. L., Madec, M., Marquis, F., Leplat, P., Paulet, J., and Boutefeu, A., 1977. Méthode rapide de caractérisation des roches mères, de leur potentiel pétrolier et de leur degré d'évolution. *Rev. Inst. Fr. Pétrole,* 32:23–42.

Goossens, H., de Leeuw, J. W., Schenk, P. A., and Brassell, S. C., 1984. Tocopherols as likely precursors of pristane in ancient sediments and crude oils. *Nature,* 312:440–442.

Henrichs, S. M., and Reeburgh, W. S., 1987. Anaerobic remineralization of marine sediment organic matter: rates and the role of anaerobic processes in the oceanic carbon economy. *J. Geomicrobiol.,* 5: 191–237.

Howarth, R. J., and Sinding-Larsen, R., 1983. Multivariate Analysis. *In* Howarth, R. J., (Ed.) *Statistics and Data Analysis in Geochemical Prospecting.* Handbook of Exploration Geology, Vol. 2. Elsevier (Amsterdam), 207–289.

Katz, B. J., 1983. Limitations of "Rock-Eval" pyrolysis for typing organic matter. *Org. Geochem.,* 4:195–199.

Mountain, G. S., and Prell, W. L., 1989. Geophysical reconnaissance for ODP Leg 117 in the northwest Indian Ocean. *In* Prell, W. D., Niitsuma, N., et al., *Proc. ODP, Init. Repts.,* 117: College Station, TX (Ocean Drilling Program), 51–64.

Nip., M., Tegelaar, E. W., de Leeuw, J. W., Schenk, P. A., and Holloway, P. J., 1986. A new non-saponifiable highly aliphatic and resistant biopolymer in plant cuticles: evidence from pyrolysis and ^{13}C-NMR analysis of present-day and fossil plants. *Naturwissenschaften,* 73:579–585.

Øygard, K., Larter, S., and Senftle, J., 1988. The control of maturity and kerogen type on quantitative analytical pyrolysis data. *Org. Geochem.* 13:1153–1162.

Pratt, L. M., Claypool, G. E., and King, J. D., 1986. Geochemical imprint of depositional conditions on organic matter in laminated-bioturbated interbeds from fine-grained marine sequences. *Mar. Geol.,* 70:67–84.

Prell, W. L., Niitsuma, N., et al., 1989. *Proc. ODP, Init. Repts.,* 117: College Station, TX (Ocean Drilling Program).

Rhoads, D. C., and Morse, J. W., 1971. Evolutionary and ecological significance of oxygen-deficient marine basins. *Lethaia,* 4:413–428.

Tarafa, M. E., Whelan, J. K., and Mountain, G. S., 1987. Sediment slumps in the Middle and Lower Eocene of Deep Sea Drilling Project Holes 605 and 613: Chemical detection by pyrolysis techniques. *In* Poag, C. W., Watts, A. B., et al., *Init. Repts. DSDP,* 95, Washington (U.S. Govt. Printing Office), 661–669.

Tegelaar, E. W., de Leeuw, J. W., Derenne, S., and Largeau, C., 1989. A reappraisal of kerogen formation. *Geochim. Cosmochim. Acta,* 53: 3103–3106.

Van de Meent, D., Brown, S. C., Philp, R. P., and Simoneit, B.R.T., 1980. Pyrolysis-high-resolution gas chromatography and pyrolysis gas-chromatography-mass spectrometry of kerogens and kerogen precursors. *Geochim. Cosmochim. Acta,* 44:999–1013.

Whelan, J. K., Kanyo, Z., Tarafa, M., and McCaffrey, M. A., 1990. Organic matter in Peru upwelling sediments—analysis by pyrolysis-GC and -GCMS. *In* Suess, E., von Huene, R., et al., *Proc. ODP, Sci. Results,* 112. College Station, TX (Ocean Drilling Program), 573–590.

Wyrtki, K., 1973. Physical oceanography of the Indian Ocean. *In* Zeitschel, B., and Gerlach, S. A. (Eds.) The *Biology of the Indian Ocean:* New York (Springer-Verlag), 18–36.

Date of initial receipt: 28 June 1989
Date of acceptance: 23 February 1990
Ms 117B-158

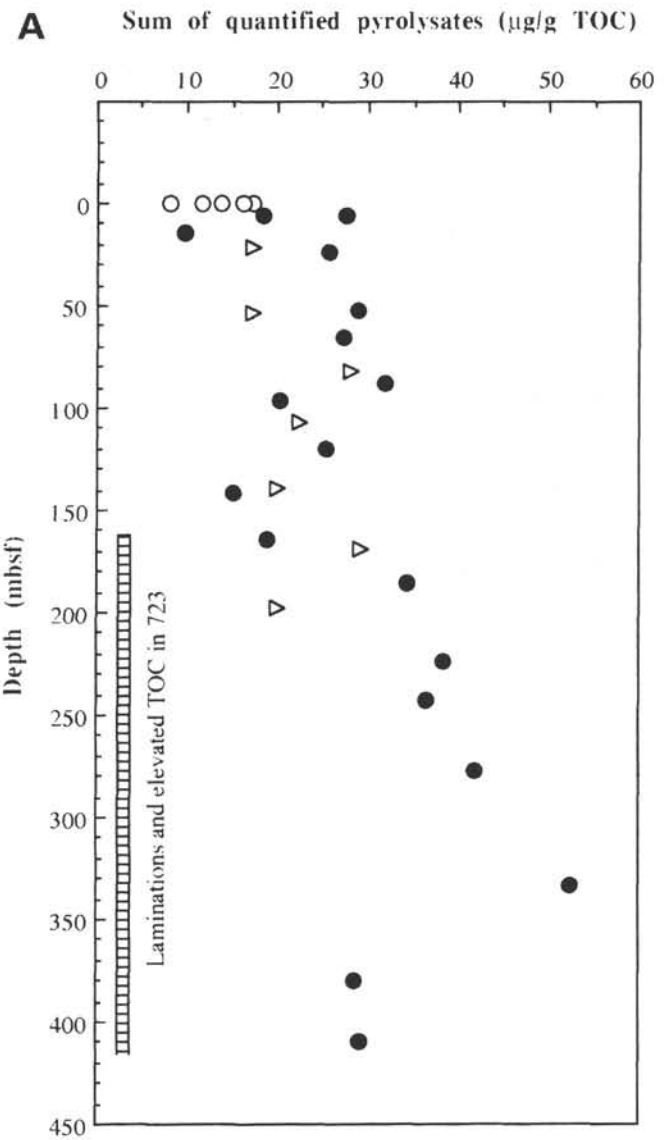

Figure 6. Downhole plots of the sum of hydrocarbons quantified in each pyrolysate **(A),** factor 1 **(B),** factor 2 **(C),** and factor 3 **(D)** with depth to show downhole variability for surface cores (circles), samples of Site 723 (dots) and 728 (triangles). The interval in Site 723 where organic carbon increases and laminations are preserved is indicated. See text for discussion.

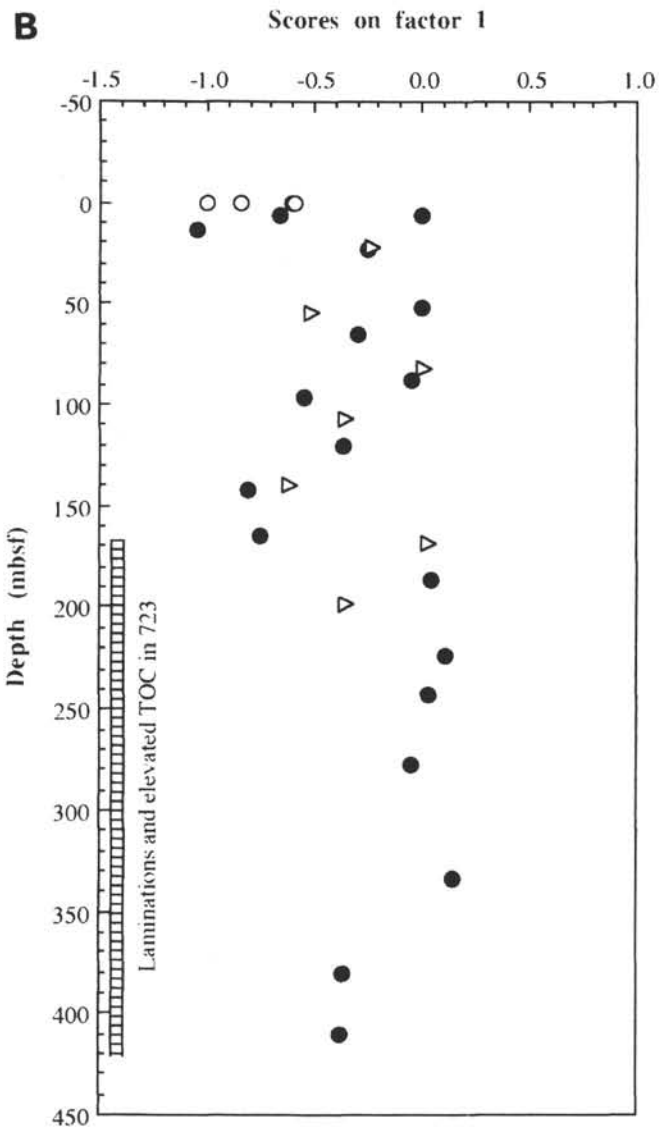

Figure 6 (continued).

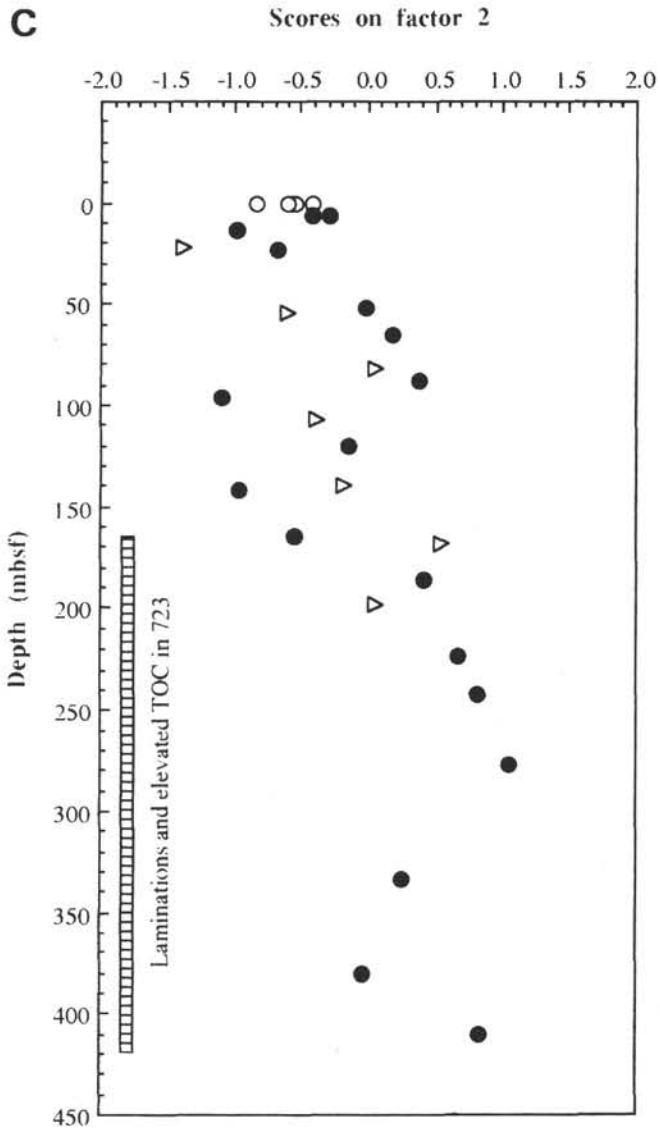

Figure 6 (continued).

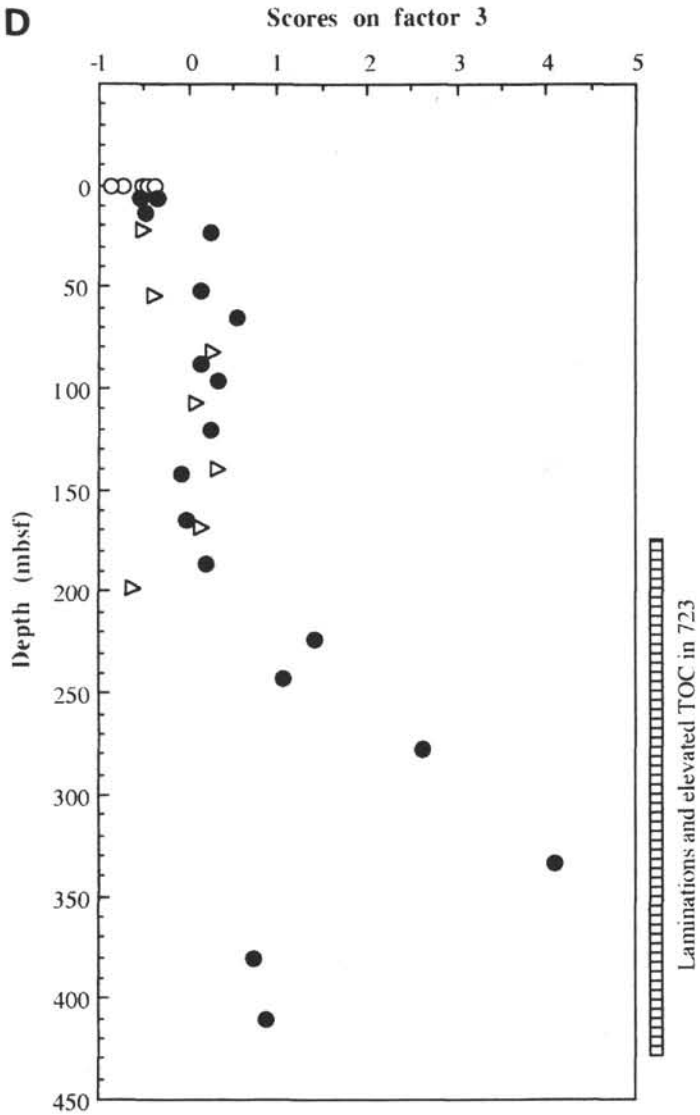

Figure 6 (continued).

Table 3. Results of pyrolysis-gas chromatography from 41 samples from surface sediments, Sites 723, 728, and 722. Results are normalized to TOC, and factor scores are given in the last columns.

Sample	Depth (mbsf)	Carbonate (%)	TOC (%)	HI CDS (mg/g TOC)	C_9-ene (μg/g TOC)	C_9-ane (μg/g TOC)	C_{10}-ane (μg/g TOC)	C_{11}-ene (μg/g TOC)	C_{11}-ane (μg/g TOC)	C_{12}-ene (μg/g TOC)
RC2709	0.0	44.0	6.50	253	772	491	334	629	932	1482
RC2712	0.0	47.0	7.40	246	0	0	293	476	697	1159
RC2714	0.0	40.0	4.70	236	0	0	315	504	830	862
RC2723	0.0	43.0	8.00	296	0	0	346	331	476	846
RC2724	0.0	64.0	2.70	318	0	0	467	889	374	515
723A-										
1H-4, 144–145 cm	5.9	50.2	1.80	647	0	0	1400	2372	1328	1072
1H-4, 145–150 cm	5.9	50.2	1.80	247	0	0	644	1589	722	889
2H-3, 149–150 cm	14.1	—	3.50	151	0	0	254	571	629	631
3H-4, 144–145 cm	23.4	56.4	0.71	289	1197	1056	775	972	1141	845
6H-4, 144–145 cm	52.3	63.9	2.04	414	1387	1127	995	2289	1201	1152
7H-2, 149–150 cm	65.5	60.5	4.50	372	1237	851	747	1131	1020	1402
9H-4, 144–145 cm	87.7	57.8	2.42	490	926	880	888	983	752	1351
11X-1, 149–150 cm	96.3	50.4	1.10	205	809	536	536	545	855	573
13X-4, 149–150 cm	119.8	63.3	3.50	397	1303	1169	560	1026	940	1223
16X-2, 149–150 cm	142.1	—	2.80	167	518	521	546	1161	579	493
18X-5, 0–1 cm	164.6	—	3.35	236	0	0	549	1343	785	740
20X-4, 0–5 cm	186.3	60.9	2.60	423	1184	1181	808	2542	1096	1308
24X-3, 0–1 cm	223.4	44.5	4.50	485	942	1133	844	1302	1264	1482
26X-3, 0–1 cm	242.8	53.2	5.60	496	1330	993	932	1568	1189	1605
29X-6, 119–120 cm	277.4	29.4	4.40	532	1257	1364	759	1648	2030	1275
36X-5, 145–150 cm	333.6	35.7	2.90	379	1362	1555	0	1148	2831	2069
38X-5, 145–150 cm	380.0	—	4.17	561	1046	947	688	2053	1014	1067
41X-2, 0–1 cm	410.0	43.0	5.50	383	1006	922	507	1289	909	944
728A-										
3H-4, 119–120 cm	21.4	57.1	1.04	233	885	721	1173	1048	808	644
6H-4, 119–120 cm	53.9	52.0	2.27	192	652	476	740	1344	793	947
9H-4, 119–120 cm	81.8	51.2	4.97	358	972	827	841	1421	1805	1000
12X-2, 119–120 cm	107.6	49.4	2.95	353	841	692	820	841	1207	834
15X-4, 119–120 cm	139.6	56.5	3.40	410	650	497	591	579	1191	938
18X-4, 119–120 cm	168.5	71.6	2.76	446	1203	899	859	1391	1699	681
21X-5, 0–1 cm	197.8	49.6	3.11	279	711	527	640	1424	1087	1248
722A-										
16X-2, 20–21 cm	146.3	86.8	0.02	2230	3500	3500	4500	5000	3500	4000
16X-2, 25–27 cm	146.4	84.1	0.44	237	1682	955	955	1614	1159	1500
16X-2, 29–30 cm	146.4	81.6	0.58	275	1776	1000	983	1810	1345	1293
16X-2, 43–44 cm	146.5	71.1	1.94	312	1835	1216	1428	2397	1577	1572
16X-2, 48–49 cm	146.6	67.1	1.93	518	2052	0	264	2295	1363	2617
16X-2, 60–61 cm	146.7	57.1	1.94	345	2005	1412	1088	2515	1309	1531
16X-2, 69–70 cm	146.8	56.6	2.06	317	1709	1291	1364	2515	1777	2398
722B-										
29-3, 140–141 cm	270.3	41.6	2.17	162	1203	959	756	1336	908	1180
29X-3, 130–131 cm	270.2	44.7	2.24	413	1013	938	1451	2634	2205	2063
29X-4, 20–21 cm	270.6	35.7	1.10	356	1664	1073	1436	1882	1609	1764
29X-4, 60–61 cm	271.0	73.0	0.27	231	1185	815	1037	1444	778	852

Table 3 (continued).

Sample	Depth (mbsf)	C_{12}-ane (μg/g TOC)	C_{13}-ene (μg/g TOC)	C_{13}-ane (μg/g TOC)	C_{14}-ene (μg/g TOC)	C_{14}-ane (μg/g TOC)	C_{15}-ene (μg/g TOC)	C_{15}-ane (μg/g TOC)	C_{16}-ene (μg/g TOC)
RC2709	0.0	429	529	343	529	282	358	403	298
RC2712	0.0	355	508	305	504	277	351	374	286
RC2714	0.0	566	536	830	998	462	451	409	264
RC2723	0.0	318	458	295	821	270	463	436	285
RC2724	0.0	296	522	270	352	226	315	204	226
723A-									
1H-4, 144–145 cm	5.9	544	2589	606	422	544	511	461	361
1H-4, 145–150 cm	5.9	406	811	306	956	528	500	372	383
2H-3, 149–150 cm	14.1	240	380	169	434	226	211	197	149
3H-4, 144–145 cm	23.4	577	1070	394	831	535	521	465	310
6H-4, 144–145 cm	52.3	637	1147	490	1353	922	696	559	446
7H-2, 149–150 cm	65.5	562	876	562	1284	824	902	660	531
9H-4, 144–145 cm	87.7	727	2070	661	1240	983	851	558	285
11X-1, 149–150 cm	96.3	364	645	609	782	473	373	309	145
13X-4, 149–150 cm	119.8	449	820	389	1011	723	709	680	526
16X-2, 149–150 cm	142.1	254	536	150	661	421	300	250	186
18X-5, 0–1 cm	164.6	337	669	221	785	537	367	331	209
20X-4, 0–5 cm	186.3	658	1027	500	1477	942	965	635	465
24X-3, 0–1 cm	223.4	558	1396	840	1829	1171	1207	1300	1000
26X-3, 0–1 cm	242.8	641	1080	634	1650	1271	1125	1096	741
29X-6, 119–120 cm	277.4	627	1382	768	1716	1273	1039	1450	927
36X-5, 145–150 cm	333.6	1928	734	1631	538	2124	1359	972	497
38X-5, 145–150 cm	380.0	530	988	408	1211	823	830	578	453
41X-2, 0–1 cm	410.0	685	1073	945	1182	975	920	1136	820
728A-									
3H-4, 119–120 cm	21.4	538	702	413	962	596	404	471	96
6H-4, 119–120 cm	53.9	414	714	330	833	551	511	467	269
9H-4, 119–120 cm	81.8	773	994	911	1199	817	891	313	414
12X-2, 119–120 cm	107.6	441	820	407	1180	786	302	380	308
15X-4, 119–120 cm	139.6	391	956	415	971	685	574	397	329
18X-4, 119–120 cm	168.5	710	1051	1344	1402	917	1004	558	558
21X-5, 0–1 cm	197.8	405	842	360	1190	685	405	521	338
722A-									
16X-2, 20–21 cm	146.3	2500	3000	1500	4000	2500	2000	1500	0
16X-2, 25–27 cm	146.4	659	1227	1341	1227	1341	1068	659	773
16X-2, 29–30 cm	146.4	724	1379	552	1586	914	776	621	466
16X-2, 43–44 cm	146.5	881	1603	784	1881	1170	1072	763	789
16X-2, 48–49 cm	146.6	1383	2591	1119	2663	1782	1922	1254	1446
16X-2, 60–61 cm	146.7	990	1077	706	1876	1211	1124	835	923
16X-2, 69–70 cm	146.8	869	1563	718	1903	1340	1398	850	850
722B-									
29-3, 140–141 cm	270.3	687	986	525	1069	751	641	677	484
29X-3, 130–131 cm	270.2	1031	2179	897	2165	1344	1232	964	920
29X-4, 20–21 cm	270.6	955	1655	2118	1964	1145	900	964	582
29X-4, 60–61 cm	271.0	630	963	556	1037	889	519	593	222

Table 3 (continued).

Sample	Depth (mbsf)	C_{16}-ane (μg/g TOC)	C_{17}-ene (μg/g TOC)	C_{17}-ane (μg/g TOC)	Prist-1-ene (μg/g TOC)	C_{18}-ene (μg/g TOC)	C_{18}-ane (μg/g TOC)	Prist-2-ene (μg/g TOC)	Pristane (μg/g TOC)
RC2709	0.0	257	337	288	411	200	335	117	15
RC2712	0.0	223	336	277	322	195	341	103	18
RC2714	0.0	228	215	389	304	151	287	130	0
RC2723	0.0	244	305	299	593	226	365	219	43
RC2724	0.0	178	181	167	193	152	244	81	30
723A-									
1H-4, 144–145 cm	5.9	272	778	100	367	300	539	594	167
1H-4, 145–150 cm	5.9	250	344	300	411	217	339	494	89
2H-3, 149–150 cm	14.1	126	303	103	149	94	197	280	31
3H-4, 144–145 cm	23.4	268	268	268	197	197	437	282	127
6H-4, 144–145 cm	52.3	368	392	480	804	348	539	539	137
7H-2, 149–150 cm	65.5	478	496	427	1151	322	513	356	162
9H-4, 144–145 cm	87.7	504	674	492	1145	492	463	331	211
11X-1, 149–150 cm	96.3	136	164	164	155	100	209	227	91
13X-4, 149–150 cm	119.8	357	343	323	717	246	400	280	120
16X-2, 149–150 cm	142.1	146	143	143	211	364	132	236	89
18X-5, 0–1 cm	164.6	203	299	328	397	236	382	573	128
20X-4, 0–5 cm	186.3	446	488	550	846	442	665	527	169
24X-3, 0–1 cm	223.4	627	618	580	1269	402	689	644	91
26X-3, 0–1 cm	242.8	618	627	727	1546	377	486	332	229
29X-6, 119–120 cm	277.4	616	582	580	1416	1105	439	768	425
36X-5, 145–150 cm	333.6	534	628	669	1228	466	614	1300	224
38X-5, 145–150 cm	380.0	367	410	444	976	400	561	444	146
41X-2, 0–1 cm	410.0	600	433	462	1264	367	725	324	289
728A-									
3H-4, 119–120 cm	21.4	96	87	115	29	19	58	0	0
6H-4, 119–120 cm	53.9	278	304	308	251	185	229	278	75
9H-4, 119–120 cm	81.8	374	473	811	652	201	221	233	171
12X-2, 119–120 cm	107.6	312	346	583	271	261	298	447	153
15X-4, 119–120 cm	139.6	326	503	421	809	344	371	462	106
18X-4, 119–120 cm	168.5	547	873	583	793	464	493	428	138
21X-5, 0–1 cm	197.8	350	714	424	148	344	386	286	177
722A-									
16X-2, 20–21 cm	146.3	0	0	0	0	0	0	1000	0
16X-2, 25–27 cm	146.4	341	636	341	0	136	227	0	136
16X-2, 29–30 cm	146.4	379	397	379	121	224	431	103	172
16X-2, 43–44 cm	146.5	588	644	613	464	608	448	402	180
16X-2, 48–49 cm	146.6	1140	1249	1264	399	850	1269	637	368
16X-2, 60–61 cm	146.7	706	686	758	314	546	799	479	227
16X-2, 69–70 cm	146.8	646	699	684	330	466	709	539	194
722B-									
29-3, 140–141 cm	270.3	516	382	373	41	157	415	230	92
29X-3, 130–131 cm	270.2	777	1045	1094	424	732	1147	612	424
29X-4, 20–21 cm	270.6	764	418	845	473	109	527	173	273
29X-4, 60–61 cm	271.0	296	74	222	0	0	185	0	37

Table 3 (continued).

Sample	Depth (mbsf)	Phytane (μg/g TOC)	Dimethyl-pyrrole (μg/g TOC)	Trimethyl thiophene (μg/g TOC)	Methyl-phenole (μg/g TOC)	Dimethyl thiophene (μg/g TOC)	Xylene (μg/g TOC)	Ethyl-methyl benzene (μg/g TOC)	Naphthalene (μg/g TOC)
RC2709	0.0	65	888	388	700	0	2682	658	923
RC2712	0.0	58	650	114	572	0	1486	561	718
RC2714	0.0	98	353	483	664	0	2515	889	968
RC2723	0.0	81	385	153	371	0	1026	691	509
RC2724	0.0	30	163	81	289	0	811	248	226
723A-									
1H-4, 144–145 cm	5.9	61	1278	933	872	0	5228	1622	889
1H-4, 145–150 cm	5.9	78	478	94	561	0	4011	1156	517
2H-3, 149–150 cm	14.1	60	686	143	369	0	1346	766	203
3H-4, 144–145 cm	23.4	85	1028	1099	394	704	5507	1789	831
6H-4, 144–145 cm	52.3	113	809	500	353	838	4289	1662	588
7H-2, 149–150 cm	65.5	84	838	1318	433	1031	4491	624	307
9H-4, 144–145 cm	87.7	145	1165	996	764	822	3701	1467	864
11X-1, 149–150 cm	96.3	55	1318	764	409	927	3800	2200	445
13X-4, 149–150 cm	119.8	111	380	360	517	689	5086	1440	500
16X-2, 149–150 cm	142.1	61	482	321	179	554	2679	1200	286
18X-5, 0–1 cm	164.6	107	699	418	678	0	3579	1257	287
20X-4, 0–5 cm	186.3	208	1127	554	742	942	5223	2042	500
24X-3, 0–1 cm	223.4	107	736	1096	644	1736	6331	3287	1096
26X-3, 0–1 cm	242.8	129	1116	816	725	1225	5766	2714	566
29X-6, 119–120 cm	277.4	77	432	923	1195	1298	6184	5070	823
36X-5, 145–150 cm	333.6	231	1321	1717	507	1372	13262	4862	672
38X-5, 145–150 cm	380.0	70	595	827	264	568	3976	2516	456
41X-2, 0–1 cm	410.0	93	791	655	755	724	3704	2476	620
728A-									
3H-4, 119–120 cm	21.4	0	981	625	413	394	1817	1423	692
6H-4, 119–120 cm	53.9	53	612	432	344	573	2181	1203	326
9H-4, 119–120 cm	81.8	64	1048	700	881	1247	3398	2247	461
12X-2, 119–120 cm	107.6	102	512	749	641	1014	3586	1661	508
15X-4, 119–120 cm	139.6	94	326	518	606	700	2612	1482	474
18X-4, 119–120 cm	168.5	101	417	728	884	888	3819	1591	942
21X-5, 0–1 cm	197.8	122	174	550	460	640	2698	1035	376
722A-									
16X-2, 20–21 cm	146.3	0	0	2000	2000	5500	12500	4500	4500
16X-2, 25–27 cm	146.4	0	0	886	818	1477	3545	1182	864
16X-2, 29–30 cm	146.4	86	310	586	776	1138	5793	1293	845
16X-2, 43–44 cm	146.5	98	778	840	830	1072	4232	1598	789
16X-2, 48–49 cm	146.6	238	1544	834	1016	902	7415		1026
16X-2, 60–61 cm	146.7	155	1253	479	789	933	5454	1552	686
16X-2, 69–70 cm	146.8	150	1612	971	850	830	3228	1466	796
722B-									
29-3, 140–141 cm	270.3	37	129	203	364	728	2922	1300	433
29X-3, 130–131 cm	270.2	330	1902	853	759	1317	3616	2067	754
29X-4, 20–21 cm	270.6	145	0	0	791	1027	3036		964
29X-4, 60–61 cm	271.0	37	222	778	704	963	6000	1222	1148

Table 3 (continued).

Sample	Depth (mbsf)	Methylfuran (μg/g TOC)	Methyl-naphthalene (μg/g TOC)	Benzo-thiophene (μg/g TOC)	Sum (mg/g TOC)	Score on Factor 1	Score on Factor 2	Score on Factor 3
RC2709	0.0	814	535	0	17.42	−0.598	−0.565	−0.507
RC2712	0.0	1719	497	0	13.78	−0.843	−0.547	−0.735
RC2714	0.0	991	381	211	16.28	−0.596	−0.602	−0.443
RC2723	0.0	83	409	175	11.52	−0.999	−0.42	−0.37
RC2724	0.0	174	270	0	8.17	−1.000	−0.837	−0.872
723A-								
1H-4, 144–145 cm	5.9	144	750	417	27.52	0.003	−0.286	−0.523
1H-4, 145–150 cm	5.9	244	567	0	18.26	−0.663	−0.418	−0.345
2H-3, 149–150 cm	14.1	143	311	266	9.67	−1.044	−0.982	−0.474
3H-4, 144–145 cm	23.4	380	704	366	25.62	−0.255	−0.678	0.258
6H-4, 144–145 cm	52.3	0	873	770	28.80	−0.005	−0.02	0.135
7H-2, 149–150 cm	65.5	296	940	389	27.25	−0.296	0.174	0.542
9H-4, 144–145 cm	87.7	2897	864	719	31.87	−0.051	0.385	0.133
11X-1, 149–150 cm	96.3	273	655	582	20.23	−0.547	−1.096	0.333
13X-4, 149–150 cm	119.8	923	660	320	25.30	−0.362	−0.139	0.262
16X-2, 149–150 cm	142.1	568	461	400	15.23	−0.805	−0.955	−0.078
18X-5, 0–1 cm	164.6	1460	624	343	18.87	−0.752	−0.537	−0.018
20X-4, 0–5 cm	186.3	2231	1154	638	34.28	0.040	0.424	0.211
24X-3, 0–1 cm	223.4	616	1173	489	38.50	0.109	0.671	1.42
26X-3, 0–1 cm	242.8	305	1536	659	36.36	0.032	0.812	1.077
29X-6, 119–120 cm	277.4	959	1127	489	42.02	−0.041	1.063	2.627
36X-5, 145–150 cm	333.6	1210	1797	928	52.29	0.146	0.246	4.105
38X-5, 145–150 cm	380.0	1566	772	566	28.56	−0.365	−0.043	0.746
41X-2, 0–1 cm	410.0	422	713	371	29.10	−0.377	0.83	0.878
728A-								
3H-4, 119–120 cm	21.4	—	721	231	17.16	−0.229	−1.374	−0.512
6H-4, 119–120 cm	53.9	—	511	251	17.43	−0.509	−0.607	−0.365
9H-4, 119–120 cm	81.8	—	853	414	28.13	0.008	0.051	0.293
12X-2, 119–120 cm	107.6	—	637	359	22.30	−0.349	−0.377	0.099
15X-4, 119–120 cm	139.6	—	579	247	20.14	−0.616	−0.188	0.326
18X-4, 119–120 cm	168.5	—	710	467	29.14	0.033	0.549	0.142
21X-5, 0–1 cm	197.8	—	582	296	20.14	−0.356	0.046	−0.623
722A-								
16X-2, 20–21 cm	146.3	0	3500	2500	79.00	5.233	−2.563	0.453
16X-2, 25–27 cm	146.4	0	1341	545	28.64	0.695	−0.092	−0.842
16X-2, 29–30 cm	146.4	0	1138	603	30.00	0.511	−0.141	−0.758
16X-2, 43–44 cm	146.5	0	1119	639	34.91	0.665	0.667	−0.482
16X-2, 48–49 cm	146.6		1306	819	45.03	0.946	3.288	−1.211
16X-2, 60–61 cm	146.7	0	897	727	36.04	0.512	1.213	−0.64
16X-2, 69–70 cm	146.8	0	1432	597	36.74	0.825	1.021	−0.802
722B-								
29-3, 140–141 cm	270.3	0	571	355	21.41	−0.102	−0.14	−0.724
29X-3, 130–131 cm	270.2	0	1388	643	40.92	0.673	2.312	−0.864
29X-4, 20–21 cm	270.6		1655	991	31.90	1.011	0.979	−1.362
29X-4, 60–61 cm	271.0	0	1074	704	25.18	0.315	−1.124	−0.489